THE JOURNAL OF BIOLOGICAL CHEMISTRY VOL. 290, NO. 18, pp. 11403–11416, May 1, 2015

Vasodilator-stimulated Phosphoprotein (VASP) Regulates Actin Polymerization and Contraction in Airway Smooth Muscle by a Vinculin-dependent Mechanism*

Received for publication, February 13, 2015, and in revised form, March 5, 2015 Published, JBC Papers in Press, March 10, 2015, DOI 10.1074/jbc.M115.645788

Yidi Wu and Susan J. Gunst[1]

From the Department of Cellular and Integrative Physiology, Indiana University School of Medicine, Indianapolis, Indiana 46202-5120

Background: The function of vasodilator-stimulated phosphoprotein (VASP) in regulating actin polymerization during airway smooth muscle contraction is unknown.
Results: VASP activity requires phosphorylation at Ser^{157}, recruitment to the membrane, and interaction with activated vinculin.
Conclusion: VASP regulates actin polymerization and contraction in smooth muscle by a unique mechanism.
Significance: The mechanism of VASP function is important for understanding actin dynamics in cells.

Vasodilator-stimulated phosphoprotein (VASP) can catalyze actin polymerization by elongating actin filaments. The elongation mechanism involves VASP oligomerization and its binding to profilin, a G-actin chaperone. Actin polymerization is required for tension generation during the contraction of airway smooth muscle (ASM); however, the role of VASP in regulating actin dynamics in ASM is not known. We stimulated ASM cells and tissues with the contractile agonist acetylcholine (ACh) or the adenylyl cyclase activator, forskolin (FSK), a dilatory agent. ACh and FSK stimulated VASP Ser^{157} phosphorylation by different kinases. Inhibition of VASP Ser^{157} phosphorylation by expression of the mutant VASP S157A in ASM tissues suppressed VASP phosphorylation and membrane localization in response to ACh, and also inhibited contraction and actin polymerization. ACh but not FSK triggered the formation of VASP-VASP complexes as well as VASP-vinculin and VASP-profilin complexes at membrane sites. VASP-VASP complex formation and the interaction of VASP with vinculin and profilin were inhibited by expression of the inactive vinculin mutant, vinculin Y1065F, but VASP phosphorylation and membrane localization were unaffected. We conclude that VASP phosphorylation at Ser^{157} mediates its localization at the membrane, but that VASP Ser^{157} phosphorylation and membrane localization are not sufficient to activate its actin catalytic activity. The interaction of VASP with activated vinculin at membrane adhesion sites is a necessary prerequisite for VASP-mediated molecular processes necessary for actin polymerization. Our results show that VASP is a critical regulator of actin dynamics and tension generation during the contractile activation of ASM.

Dynamic remodelling of the actin cytoskeleton is recognized as an important step in the agonist-induced activation of contraction and tension development in airway smooth muscle (ASM)[2] and in other smooth muscle tissues (1). The regulation of actin filament remodelling is a complex process involving the coordinated activity of multiple proteins; but the molecular mechanisms for actin remodelling and the processes by which actin regulatory proteins are activated in response to contractile and dilatory agents in smooth muscle tissues are poorly understood. In ASM, neuronal Wiskott-Aldrich syndrome protein (N-WASp) plays a critical role in the initiation of actin polymerization during contractile stimulation by activating the Arp2/3 complex (2). The Arp2/3 complex is believed to nucleate the formation of new actin filaments that branch off the sides of existing filaments (3). However, the importance of other catalysts for actin polymerization in regulating the contraction of ASM has not been determined.

Members of the Ena/VASP family regulate cell motility and shape in a wide variety of cell types (4, 5). Although a number of molecular functions that affect actin dynamics have been attributed to Ena/VASP proteins, there is extensive evidence for their role as actin filament elongation factors, *i.e.* they bind to the barbed (fast growing) ends of existing actin filaments and promote filament lengthening (4, 6, 7). The mechanism for the elongation of actin filaments by VASP is proposed to require the assembly of VASP into tetrameric oligomers and the membrane recruitment and anchoring of VASP to the scaffolding proteins vinculin and zyxin at sites of actin filament assembly. Filament elongation can then occur via the recruitment of profilin-G actin complexes to bind to VASP tetramers, followed by the transfer and assembly of G-actin monomers into the barbed ends of the actin filaments that are also bound to VASP (8–10). We evaluated ASM for evidence of a VASP-mediated process of actin elongation during contractile and dilatory stimulation.

Ena/VASP proteins consist of 3 domains, N- and C-terminal Ena/VASP homology 1 and 2 (EVH) domains and a central

* This work was supported, in whole or in part, by National Institutes of Health Grants R01 HL29289, HL074099, and R01HL109629.
[1] To whom correspondence should be addressed: 635 Barnhill Dr., Indianapolis, IN 46202. Tel.: 317-274-4108; E-mail: sgunst@iupui.edu.

[2] The abbreviations used are: ASM, airway smooth muscle; N-WASp, neuronal Wiskott-Aldrich syndrome protein; EVH, Ena/VASP homology; BIM I, bisindolylmaleimide I; TES, *N*-tris(hydoxymethyl)methyl-2-aminoethanesulfonic acid; PLA, proximity ligation assay; ACh, acetylcholine; FSK, forskolin; MLC, myosin light chain; VASP, vasodilator-stimulated phosphoprotein; EGFP, enhanced green fluorescent protein .

proline-rich region (4, 7). The EVH1 domain contains binding sites for several focal adhesion scaffolding proteins including vinculin; the proline-rich region contains binding sites for profilin-actin, a primary source of actin monomers for actin filament polymerization; and the EVH2 domain contains binding sites for filamentous (F)- and globular (G)-actin. The C-terminal coiled-coil region within the EVH2 domain of VASP mediates the assembly of VASP monomers into stable tetramers, believed to be an essential step for VASP to function as an elongation factor (4, 8, 11–15). Ena/VASP proteins are also known substrates for both serine/threonine and tyrosine kinases (16–18). The phosphorylation of VASP Ser^{157} has been implicated in the cellular localization of VASP (17, 19). VASP plays a role in the regulation of actin polymerization and contraction in aortic smooth muscle (20). VASP is expressed in ASM tissues and undergoes phosphorylation at Ser^{157} during β adrenergic stimulation (21, 22); but the function of VASP during the contraction and relaxation of ASM is unknown.

Signaling events that regulate actin polymerization during contractile stimulation of ASM are mediated by adhesome complexes at integrin-ECM adhesion junctions (23). Vinculin, a VASP ligand, plays an important structural role in these junctions by binding to the integrin-binding proteins talin and α-actinin as well as to actin filaments (24). Vinculin can assume a closed conformation in which it does not bind to actin or talin, and an open conformation in which its actin and talin binding sites are exposed (25, 26). The contractile stimulation of ASM tissues with ACh induces the recruitment of vinculin to membrane adhesion complexes and its activation to an open ligand-binding conformation (27, 28). Vinculin phosphorylation on Tyr^{1065} is necessary for vinculin to sustain an activated conformation in which it can bind to talin and actin filaments (27). VASP has been shown to bind to the proline-rich hinge region of vinculin at cell junctions (29–31); thus we hypothesized that vinculin might play a role in the regulation of VASP-mediated actin dynamics in ASM. To test this hypothesis, we evaluated the molecular mechanisms by which contractile and dilatory stimuli regulate the activity of VASP and its interaction with vinculin in ASM.

Our results suggest that VASP functions as an actin elongation factor at the ASM plasma membrane, and that the interaction of VASP with activated vinculin is prerequisite to this function. We conclude that VASP is an important catalyst for actin polymerization during the contraction of ASM tissues.

EXPERIMENTAL PROCEDURES

Preparation of Smooth Muscle Tissues and Measurement of Force—Mongrel dogs were euthanized in accordance with the guidelines of the Institutional Animal Care and Use Committee (IACUC), Indiana University School of Medicine. The trachea was immediately removed and immersed in physiological saline solution at 22 °C. The solution was aerated with 95% O_2, 5% CO_2 to maintain a pH of 7.4. Rectangular strips of tracheal muscle 1 mm in diameter and 10 mm in length were dissected after removal of the epithelium and connective tissue layer. Each muscle strip was placed in physiological saline solution at 37 °C in a 25-ml organ bath and attached to a Grass force transducer for the measurement of force. At the beginning of each experiment, muscle length was progressively increased until the force of active contraction in response to a contractile stimulus reached a maximum (optimal length).

Reagents and Antibodies—Antibodies used in these experiments were: mouse monoclonal human VASP (BD Biosciences Pharmingen), rabbit polyclonal human VASP (Cell Signaling), mouse monoclonal human VASP phospho-Ser^{157} (Abcam), mouse monoclonal human VASP phospho-Ser^{239} (Millipore); rabbit polyclonal human VASP phospho-Ser^{239} (Cell Signaling); rabbit polyclonal GFP (MBL); rabbit His tag (Cell Signaling), rabbit polyclonal bovine myosin light chain, custom made by BABCO (Richmond, CA); polyclonal vinculin (against canine cardiac vinculin); mouse monoclonal human profilin1 (Abcam); rabbit polyclonal human profilin (Cytoskeleton); mouse monoclonal human actin (Sigma); Alexa Fluor 488 and 546 (Invitrogen); and IRDye 800CW goat anti-mouse IgG and IRDye 680LT goat anti-rabbit IgG (Li-Cor).

Reagents included the Duolink *in situ* proximity ligation kit (PLA) and anti-mouse plus and anti-rabbit minus probes (Olink Bioscience, Uppsala, Sweden), lysis and F-actin stabilization buffers (Cytoskeleton), and protein kinase C inhibitor bisindolylmaleimide I (BIM) (Sigma). Plasmid vectors used included pcDNA3 EGFP full-length human VASP and VASP S157A (alanine substituted at Ser^{157}, His_6 tagged) (17, 18), pEGFP-vinculin full-length chicken vinculin (residues 1–1066) (32), and non-phosphorylatable vinculin Y1065F (27).

Introduction of Plasmids into Tracheal Smooth Muscle Tissues—Plasmids encoding full-length EGFP VASP and EGFP VASP S157A were introduced into the smooth muscle strips by the method of reversible permeabilization as previously described (2, 33–36). Muscle tissues were attached to a metal hooks and incubated successively in each of the following solutions: Solution 1, which contained 10 mM EGTA, 5 mM Na_2ATP, 120 mM KCl, 2 mM $MgCl_2$, and 20 mM TES (at 4 °C, pH 7.1, 100% O_2 for 120 min); solution 2, which contained 0.1 mM EGTA, 5 mM Na_2ATP, 120 mM KCl, 2 mM $MgCl_2$, and 20 mM TES and 10 μg/ml of plasmids (at 4 °C, pH 7.1, overnight); solution 3, which contained 0.1 mM EGTA, 5 mM Na_2ATP, 120 mM KCl, 10 mM $MgCl_2$, and 20 mM TES (at 4 °C, pH 7.1, 100% O_2 for 30 min); and solution 4, which contained 110 mM NaCl, 3.4 mM KCl, 0.8 mM $MgSO_4$, 25.8 mM $NaHCO_3$, 1.2 mM KH_2PO_4 (at 22 °C, pH 7.4, for 60 min and aerated with 95% O_2 and 5% CO_2). After 30 min in solution 4, $CaCl_2$ was added gradually to reach a final concentration of 2.4 mM. The plasmid-treated tissue strips were then incubated at 37 °C for 2 days in DMEM containing 5 mM Na_2ATP, 100 units/ml of penicillin, 100 μg/ml of streptomycin, and 10 μg/ml of plasmids to allow for expression of the recombinant proteins. Sham-treated tissues were subjected to identical procedures except that no plasmids were included in Solution 2. Tissues were then quickly frozen using liquid N_2-cooled tongs for biochemical analysis or dissociated for cellular imaging studies.

Immunoblot and Immunoprecipitation—Frozen muscle tissues were pulverized, and the proteins were extracted for electrophoresis or immunoprecipitation as previously described (2, 28). For immunoprecipitation, the extracts were precleared at 4 °C with protein A/G UltraLink Resin and incubated with antibodies against the target protein. Western blotting of immuno-

precipitates or muscle extracts was performed to quantitate proteins. The proteins were visualized by ECL and digitally quantified using a Bio-Rad ChemiDoc XRS detection system, VASP phosphorylation at Ser^{157} was quantitated by probing membranes simultaneously with mouse anti-phospho-Ser^{157} VASP Ab (Abcam) and polyclonal rabbit anti-VASP Ab (Cell Signaling), and then using fluorescent probes to detect both antibodies simultaneously using a Li-Cor Odyssey infrared imaging system.

Myosin Light Chain Phosphorylation—Muscle strips were rapidly frozen and then immersed in acetone containing 10% (w/v) trichloroacetic acid and 10 mM DTT that was precooled with dry ice. Strips were thawed in acetone/trichloroacetic acid/DTT at room temperature and then washed 4 times with acetone/DTT. Proteins were extracted for 2–3 h in 8 M urea, 20 mM Tris base, 22 mM glycine, and 10 mM DTT. Myosin light chains (MLCs) were separated by glycerol-urea polyacrylamide gel electrophoresis, transferred to nitrocellulose, and incubated with polyclonal rabbit MLC 20 antibody (2, 37, 38). Unphosphorylated and phosphorylated bands of MLCs were visualized by ECL and quantified by densitometry. MLC phosphorylation was calculated as the ratio of phosphorylated MLCs to total MLCs for each sample.

Cell Dissociation and Analysis of Protein Localization—Smooth muscle cells were enzymatically dissociated from tracheal muscle strips, plated onto glass slides, and allowed to adhere for 60 min as previously described (2, 35). After cells were stimulated with ACh, FSK, or left unstimulated, cells were then fixed and visualized for EGFP fluorescence or stained for immunofluorescence analysis. The effects of stimulation with ACh or FSK on the localization of proteins were evaluated in freshly dissociated smooth muscle cells using a Zeiss LSM 510 confocal microscope. Images of smooth muscle cells were analyzed for regional differences in fluorescence intensity by quantifying the pixel intensity with a series of cross-sectional line scans along the entire length of each cell, excluding the nucleus (2, 35). The ratio of pixel intensity between the cell periphery and the cell interior was computed for each line scan by calculating the ratio of the average maximum pixel intensity at the cell periphery to the average minimum pixel intensity in the cell interior. The ratios of pixel intensities between the cell periphery and the cell interior for all line scans performed on a given cell were averaged to obtain a single value for each cell.

In Situ Proximity Ligation Assay—In situ proximity ligation assays were performed to detect interactions between VASP and vinculin, VASP and profilin, VASP-VASP complexes, and phospho-Ser^{157} VASP in dissociated cells. PLA provides a method for the precise detection of protein-protein complexes or interactions and protein modifications. Two primary antibodies against the target proteins or protein epitopes are raised in different species, and a pair of oligonucleotide-labeled secondary antibodies (+ and − PLA probes) are targeted to each pair of primary antibodies. The probes form circular DNA strands only when they are bound in very close proximity (<40 nm). These DNA circles serve as templates for localized rolling circle amplification, generating a fluorescent signal (spot) that enables individual interacting pairs of the target protein molecules to be visualized. The PLA signal thus allows for the detection of a complex between two target proteins at a very high resolution (39, 40).

Smooth muscle cells were fixed, permeabilized, and incubated with a pair of primary antibodies of different species against two target proteins followed by a pair of oligonucleotide-labeled secondary antibodies (Duolink + and − PLA probes). Mouse anti-VASP and rabbit anti-vinculin antibodies were used to probe VASP-vinculin interactions, rabbit anti-VASP and mouse anti-profilin antibodies were used to probe VASP-profilin interactions, rabbit anti-VASP and mouse anti-VASP phospho-Ser^{157} antibodies were used to detect VASP phospho-Ser^{157}, and mouse and rabbit phospho-Ser^{239} VASP antibodies were used to detect VASP-VASP interactions. PLA probe hybridization, ligation, amplification, and detection media were administered according to the manufacturer's instructions (Olink Bioscience). Cells from unstimulated and ACh- or FSK-stimulated groups were analyzed for interactions by counting PLA fluorescent spots using a Zeiss LSM510 confocal microscope. Duolink ImageTool software was used to quantitate PLA signals.

Analysis of F-actin/G-actin Ratio—The concentration of F-actin and G-actin in smooth muscle tissues was measured using an assay kit from Cytoskeleton Inc. Each of the smooth muscle strips was homogenized in F-actin stabilization buffer. The supernatants of protein extracts (G-actin fraction) were collected after high speed centrifugation at 150,000 × *g* for 60 min at 37 °C. The pellets were resuspended in ice-cold distilled H_2O plus 10 μM cytochalasin D and then incubated on ice for 1 h to dissociate F-actin. The supernatant of the resuspended pellets was collected after centrifugation at 4 °C. Equal volumes of the first supernatant (G-actin) or second supernatant (F-actin) were subjected to analysis by immunoblot using anti-actin antibody. The amount of F-actin and G-actin was determined by densitometry and the ratio of F-actin to G-actin was used for the analysis.

Statistics—Data are expressed as mean ± S.E. Differences between treatment groups were determined using paired or unpaired two-tailed Student's *t* test or analysis of variance. Differences were considered statistically significant when $p < 0.05$.

RESULTS

Stimulation with ACh, FSK, or Epinephrine Induces VASP Phosphorylation at the Cell Membrane in ASM—VASP phosphorylation at Ser^{157} was measured in ASM tissues stimulated with 10^{-4} or 10^{-5} M ACh for time periods up to 30 min (Fig. 1*A*). The shift in apparent molecular mass of VASP from 46 to 50 kDa by SDS-PAGE was used to analyze stoichiometric changes in the phosphorylation of VASP at Ser^{157}. We confirmed that the 50-kDa band was serine 157-phosphorylated VASP by simultaneously probing each membrane using a site-specific VASP phospho-Ser^{157} antibody (Fig. 1, *A* and *B*) (41). Tissues were also stimulated with FSK for up to 20 min to evaluate VASP phosphorylation at Ser^{157} (Fig. 1, *A* and *B*). VASP Ser^{157} phosphorylation increased significantly with both ACh and FSK stimulation, approaching a maximum by 10 min (Fig. 1*C*). FSK induced significantly higher levels of VASP Ser^{157} phosphorylation than ACh. Stimulation of muscles with the adrenergic hormone epinephrine affected VASP Ser^{157} phosphory-

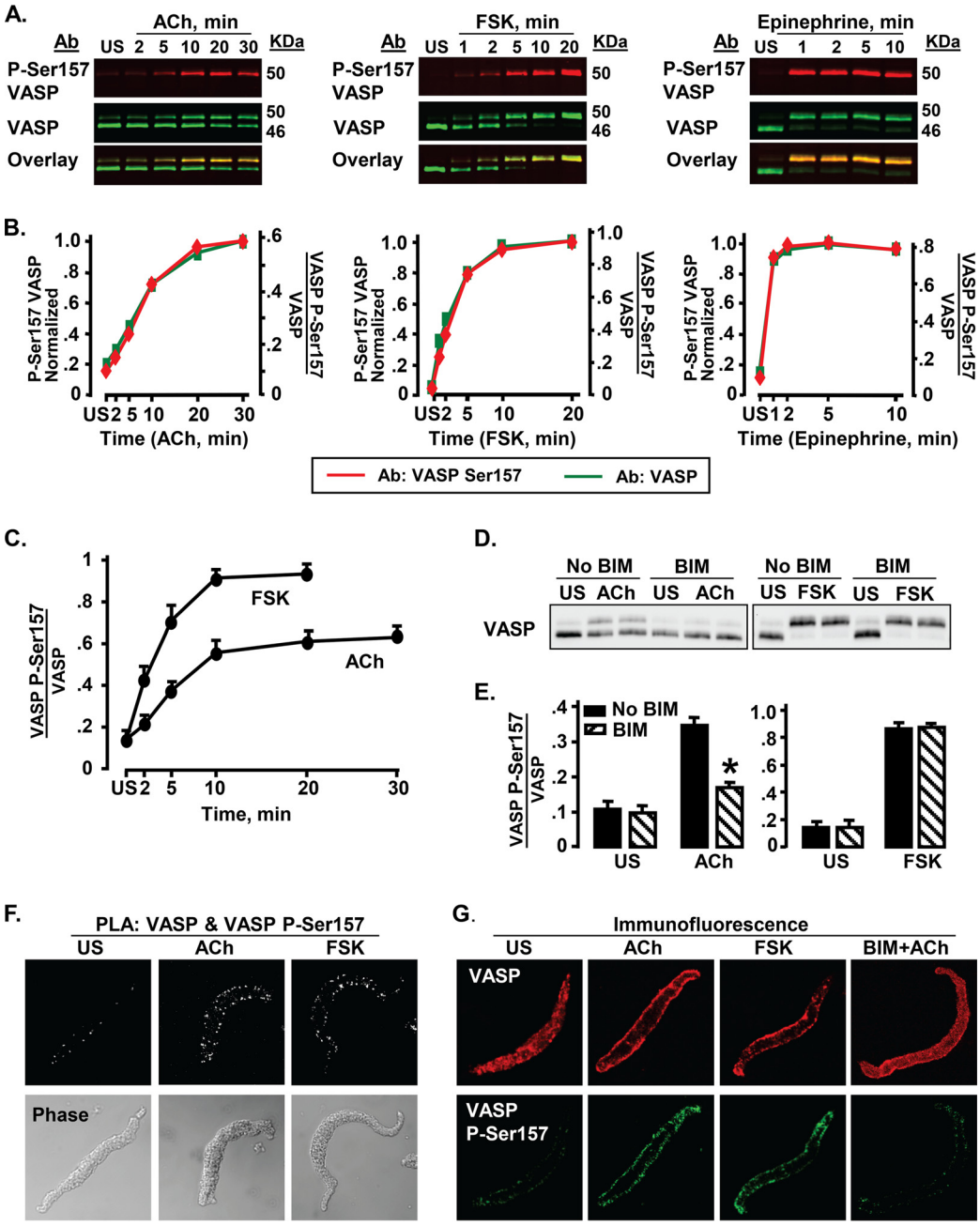

FIGURE 1. **VASP Ser^{157} phosphorylation (VASP P-Ser^{157}) increases during stimulation with ACh, FSK, and epinephrine in ASM tissues.** *A*, immunoblots of VASP and phospho-Ser^{157} VASP from extracts of muscle tissues either unstimulated (*US*) or stimulated with 10^{-4} M ACh for time periods up to 30 min. Phosphorylation of VASP on Ser^{157} was probed concurrently with VASP phospho-Ser^{157} and VASP antibodies. Probes were visualized using a Li-Cor Odyssey imaging system. Ser^{157}-phosphorylated VASP migrated concurrently with the 50-kDa VASP band (overlay). *B,* VASP Ser^{157} phosphorylation calculated from VASP (*green*) and VASP phospho-Ser^{157} (*red*) immunoblots overlay very closely. In the VASP immunoblot, Ser^{157} phosphorylation was calculated from the ratio of the upper VASP 50-kDa band to total VASP (both 50- and 46-kDa bands). In the VASP phospho-Ser^{157} immunoblot, VASP Ser^{157} phosphorylation was calculated from the phospho-Ser^{157} VASP band normalized to both VASP bands (46 and 50 kDa). For each stimulus agent, VASP Ser^{157} phosphorylation determined from VASP phospho-Ser^{157} immunoblot was normalized to maximum VASP Ser^{157} phosphorylation. *C,* mean increases in VASP Ser^{157} phosphorylation in response to stimulation with ACh ($n = 13$–20) or FSK ($n = 14$) at each time point. Both FSK and ACh cause significant increases in VASP Ser^{157} phosphorylation at all time points after stimulation; the increase in VASP Ser^{157} phosphorylation stimulated by FSK is significantly higher than that caused by ACh at all time points ($p < 0.05$). *D* and *E,* immunoblots and mean results for VASP Ser^{157} phosphorylation in tissues treated or not treated with 10 μM of the PKC inhibitor BIM and stimulated with 10^{-5} M ACh or 10^{-6} M FSK. BIM causes significant inhibition of ACh stimulated but not FSK stimulated VASP Ser^{157} phosphorylation. *, significantly different from corresponding *No BIM* tissues ($n = 6$). *F, in situ* PLA performed in freshly dissociated ASM cells using VASP phospho-Ser^{157} and VASP antibodies to determine the localization of phospho-Ser^{157} VASP. Cells were stimulated with 10^{-4} M ACh, 10^{-6} M FSK, or left unstimulated. Phospho-Ser^{157} VASP localizes at the ASM cell membrane in response to stimulation with either ACh or FSK. Each fluorescent spot indicates Ser^{157}-phosphorylated VASP. More spots are seen at the membrane of the ACh- or FSK-stimulated cells than of US cells. Results are representative of observations in 37 ACh-stimulated cells, 26 FSK-stimulated cells, and 33 US cells. *G,* localization of phospho-Ser^{157} VASP and total VASP in freshly dissociated ASM cells stimulated with 10^{-4} M ACh, 10^{-6} M FSK, 10^{-4} M ACh and BIM, or US, and double stained for VASP and phospho-Ser^{157} VASP. VASP is found both at the membrane and in the cytoplasm of ACh-stimulated, FSK-stimulated, and US cells, but is more concentrated at the membrane of the stimulated cells. Phospho-Ser^{157} VASP is observed only on the cell membrane in US, ACh-, and FSK-stimulated cells. BIM treatment inhibits VASP recruitment to the membrane and decreases ACh-induced VASP Ser^{157} phosphorylation, but does not affect the localization of Ser^{157}-phosphorylated VASP on the membrane. Representative results are from 55 US cells, 47 ACh-stimulated cells, 26 FSK-stimulated cells, and 15 ACh-stimulated cells treated with BIM.

lation similarly to FSK, but with a somewhat more rapid time course (Fig. 1, *A* and *B*).

The PKC inhibitor BIM (42) was used to determine whether PKC is involved in the regulation of VASP Ser^{157} phosphorylation in response to ACh or FSK. Tracheal smooth muscle tissues were treated with 10 μM BIM and then stimulated with ACh or FSK (Fig. 1, *D* and *E*). BIM treatment significantly suppressed ACh-induced VASP Ser^{157} phosphorylation but it did not affect VASP phosphorylation stimulated by FSK, indicating that PKC mediates VASP Ser^{157} phosphorylation in response to stimulation with ACh but not FSK.

The cellular localization of phospho-Ser^{157} VASP was analyzed by PLA using probes against antibodies for phospho-Ser^{157} VASP and VASP. Close proximity (<40 nm) of the target epitopes on VASP results in the generation of a fluorescent spot indicating VASP phosphorylation. Phospho-Ser^{157} VASP was observed on the membrane of unstimulated and ACh- or FSK-stimulated cells; however, many more spots were observed in cells stimulated with ACh or FSK than in unstimulated cells (Fig. 1*F*).

Immunofluorescence was used to evaluate the localization of phospho-Ser^{157} VASP and total VASP in freshly dissociated cells (Fig. 1*G*). In both unstimulated cells and cells stimulated with ACh or FSK, phospho-Ser^{157} VASP was only detected at the cell membrane, whereas VASP was detected in both the cytoplasm and at the cell membrane. The intensity of phospho-Ser^{157} VASP fluorescence was much higher in ACh- or FSK-stimulated cells than in unstimulated cells. Treatment with BIM markedly reduced VASP phospho-Ser^{157} fluorescence in ACh-stimulated cells and inhibited VASP localization to the membrane (Fig. 1*G*).

Inhibition of VASP Ser^{157} Phosphorylation Inhibits ACh-induced Smooth Muscle Contraction and Actin Polymerization, but It Does Not Affect MLC Phosphorylation—His-EGFP VASP S157A or His-EGFP VASP WT was expressed in ASM tissues and force in response to 10^{-5} M ACh measured after expression (Fig. 2, *A*–*C*). VASP S157A does not undergo phosphorylation at Ser^{157} due to the substitution of alanine for serine (Fig. 2*C*). The expression of VASP S157A in ASM tissues significantly depressed endogenous VASP Ser^{157} phosphorylation and inhibited contractile force in response to 10 min stimulation with ACh (Fig. 2, *A*–*E*). Neither sham treatment nor expression of VASP WT affected force or VASP Ser^{157} phosphorylation in response to ACh.

The proportions of F-actin to G-actin were analyzed in unstimulated and ACh-stimulated muscle tissues expressing VASP S157A, VASP WT, or sham-treated tissues (Fig. 2*F*). Expression of VASP S157A prevented the increase in the F- to G-actin ratio in response to stimulation with ACh; whereas expression of VASP WT or sham treatment had no significant effect on actin polymerization in response to ACh. ACh stimulation increased actin polymerization in tracheal muscle tissues, whereas stimulation with FSK did not (Fig. 2*G*).

MLC phosphorylation was analyzed in unstimulated and ACh-stimulated muscle tissues expressing VASP S157A, VASP WT, or sham-treated tissues (Fig. 2, *H* and *I*). MLC phosphorylation in response to ACh stimulation increased significantly regardless of treatment and was not significantly different among tissues expressing VASP WT, VASP S157A, or sham-treated tissues.

ACh Stimulates the Recruitment of VASP and Vinculin to the Membrane and the Formation of VASP-Vinculin Complexes; FSK Stimulates the Membrane Recruitment of VASP but Not Vinculin—Co-immunoprecipitation analysis was used to assess the interaction of VASP with vinculin in tissues stimulated with ACh or FSK (Fig. 3*A*). Stimulation with ACh significantly increased the amount of vinculin that co-precipitated with VASP compared with unstimulated tissues (Fig. 3*B*). In contrast, stimulation with FSK did not significantly increase the co-precipitation of vinculin with VASP.

The effects of ACh and FSK on the interaction of VASP and vinculin were also evaluated using PLA in cells freshly dissociated from ASM tissues (Fig. 3, *C* and *D*). Significantly more PLA spots indicating VASP-vinculin complexes were observed in ACh-stimulated cells than in FSK-stimulated or unstimulated cells.

The colocalization of VASP and vinculin was evaluated by double immunofluorescence staining. Smooth muscle cells were freshly dissociated from tracheal smooth muscle tissues and stimulated for 10 min with ACh or FSK or left unstimulated. In unstimulated cells, both VASP and vinculin were distributed throughout the cell cytoplasm and at the membrane. In cells stimulated with ACh, VASP and vinculin were co-localized at the cell membrane, and little fluorescence was observed in the cytoplasm for either protein. In cells stimulated with FSK, VASP was localized almost entirely at the membrane, whereas vinculin was distributed throughout the cytoplasm (Fig. 3*E*). The effect of FSK and ACh on the distribution of VASP and vinculin to the membrane *versus* the cytoplasm was analyzed in 65 cells from 3 separate experiments (Fig. 3*F*). ACh stimulation significantly increased the membrane localization of both VASP and vinculin. In contrast, FSK stimulated the membrane localization of VASP but not vinculin.

VASP Ser^{157} Phosphorylation Is Required for VASP Recruitment to the Membrane and Its Interaction with Vinculin in Membrane Protein Complexes—The role of VASP Ser^{157} phosphorylation in the cellular localization of VASP was evaluated by analyzing the localization of EGFP VASP S157A and EGFP VASP WT in dissociated cells stimulated with either ACh or FSK (Fig. 4). Stimulation with either ACh or FSK caused the recruitment of EGFP VASP WT to the membrane, but neither ACh nor FSK stimulated the recruitment of EGFP VASP S157A to the membrane (Fig. 4, *A* and *B*). The amount of EGFP VASP WT at the membrane was significantly higher in cells stimulated with ACh or FSK than in unstimulated cells (Fig. 4*B*).

PLA was used to evaluate the effect of VASP Ser^{157} phosphorylation on the interaction of vinculin and VASP (Fig. 4, *C* and *D*). In unstimulated freshly dissociated smooth muscle cells expressing VASP WT or VASP S157A, very few PLA spots were observed in the cell, indicating few protein complexes containing both VASP and vinculin. In cells expressing VASP WT, stimulation with ACh caused a significant increase in the number of PLA spots at the cell membrane, indicating that ACh stimulated the formation of VASP-vinculin protein complexes. The expression of VASP S157A significantly inhibited the for-

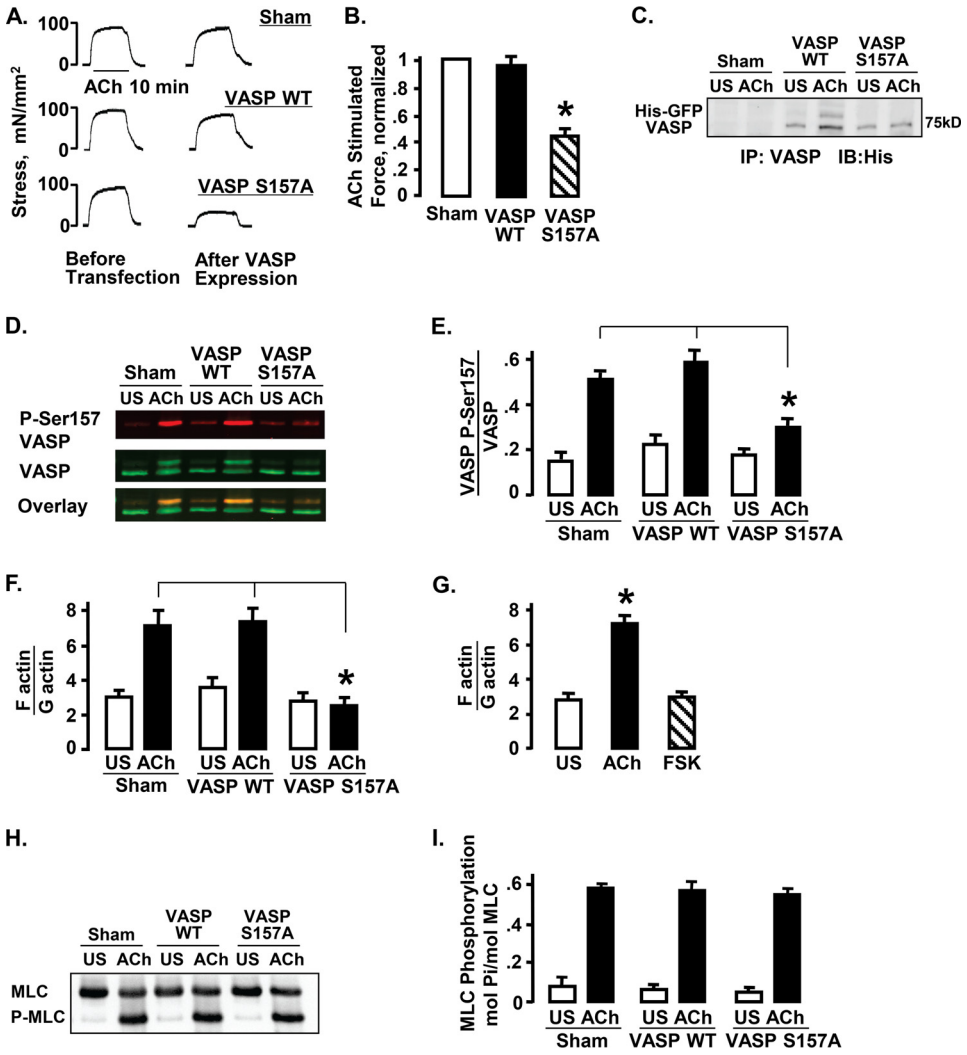

FIGURE 2. **Expression of VASP S157A in ASM tissues inhibits ACh-stimulated contractile force and actin polymerization, but it does not affect MLC phosphorylation.** *A,* active stress in ASM tissues in response to stimulation with 10^{-5} M ACh before and after expression of His-EGFP VASP WT, His-EGFP VASP S157A, or sham transfection. *B,* expression of His-EGFP VASP S157A significantly depressed the force relative to sham-treated tissues, but expression of His-EGFP VASP WT had no significant effect. ACh-stimulated force normalized to maximal force in sham-treated tissues. *, significantly different from sham-treated tissues ($n = 9$). *C,* immunoblot against the His epitope of VASP immunoprecipitates from ACh-stimulated or unstimulated (*US*) tissues expressing His-EGFP VASP WT, His-EGFP VASP S157A, or sham treated. Expression of recombinant His-EGFP VASP and His-EGFP VASP S157A was observed in transfected tissues but not sham-treated tissues. *D,* immunoblot against VASP and VASP phospho-Ser^{157} from tissues transfected with His-EGFP VASP WT, His-EGFP VASP S157A, or sham treated. *E,* expression of VASP S157A significantly inhibited endogenous VASP Ser^{157} phosphorylation in response to 10^{-5} M ACh stimulation ($n = 11$ for sham and VASP S157A, $n = 6$ for VASP WT). *, significantly different from sham-treated tissues. *F,* actin polymerization was determined in tissues expressing VASP S157A, VASP WT, or sham treated. Actin polymerization increases in response to ACh in sham-treated and VASP WT-treated muscle tissues but not in tissues expressing VASP S157A. *, significantly different ($n = 11$ for sham and VASP S157A, $n = 5$ for VASP WT). *G,* actin polymerization was determined in tissues stimulated with ACh, FSK, or US. Actin polymerization was significantly increased in response to ACh stimulation but not with FSK stimulation ($n = 4$). *H* and *I*, MLC phosphorylation measured by urea gel electrophoresis in US or ACh-stimulated tissues expressing VASP S157A, VASP WT, or sham treated. There were no significant differences in MLC phosphorylation among ACh-stimulated or US tissues subjected to different treatments ($n = 5$).

mation of VASP-vinculin protein complexes in response to ACh.

Co-immunoprecipitation analysis was also used to evaluate the interaction of vinculin and VASP in tissues expressing VASP WT or VASP S157A. The amount of vinculin that co-precipitated with VASP increased significantly in response to ACh stimulation in sham-treated tissues and tissues expressing VASP WT, but not in tissues expressing VASP S157A (Fig. 4, *E* and *F*). Thus, the expression of VASP S157A significantly inhibited the formation of VASP-vinculin protein complexes in response to ACh in both tissues and isolated dissociated cells, demonstrating that the Ser^{157} phosphorylation of VASP and its membrane localization are necessary for the interaction of VASP with vinculin.

Vinculin Tyr^{1065} Phosphorylation and Activation Are Required for the Formation of VASP-Vinculin Protein Complexes at the Membrane—We previously demonstrated that vinculin phosphorylation at Tyr^{1065} is required for vinculin to maintain an open activated conformation (27). Smooth muscle tissues were stimulated with FSK for 10 min or ACh for 5 min, then vinculin Tyr^{1065} phosphorylation and VASP phosphorylation were analyzed by immunoblot (Fig. 5). Stimulation with ACh, but not with FSK, induced vinculin Tyr^{1065} phosphorylation, indicating that vinculin undergoes activation in response

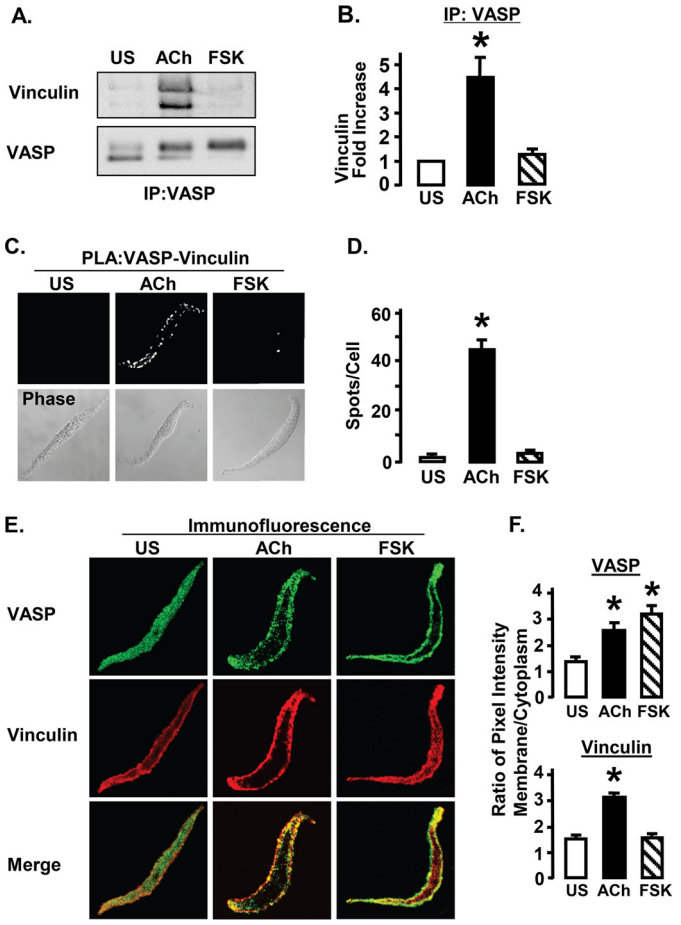

FIGURE 3. **VASP forms complexes with vinculin at the membrane of ASM cells in response to stimulation with ACh but not FSK.** *A,* vinculin immunoprecipitates with VASP from extracts of ACh stimulated but not FSK stimulated or US tissues. *B*, vinculin co-immunoprecipitation with VASP was significantly greater in extracts from ACh-stimulated than from FSK-stimulated or US tissues. *, significantly different from US ($n = 9$). *C*, interaction of vinculin and VASP in freshly dissociated ASM cells was visualized by *in situ* PLA using VASP and vinculin antibodies. Each fluorescent spot indicates complex between vinculin and VASP. PLA spots are observed at the membrane of the ACh-stimulated cells, whereas very few spots are observed in FSK-stimulated or US cells. *D,* mean number of PLA spots was significantly higher in ACh-stimulated smooth muscle cells than in FSK-stimulated or US cells. *, significantly higher than US ($n = 27–35$ cells). *E,* immunofluorescence images of dissociated cells stimulated with ACh, FSK, or left unstimulated (*US*) and then double stained for VASP (*green*) and vinculin (*red*). ACh increases the localization of both VASP and vinculin at the cell membrane. FSK increases the localization of VASP at the cell membrane, but has little effect on vinculin localization. Merged images show colocalization of VASP and vinculin in *yellow*. *F,* mean ratios of membrane to cytoplasmic pixel intensity for VASP and vinculin. The ratio of membrane to cytoplasmic VASP localization is significantly higher in ACh ($n = 28$)- and FSK ($n = 15$)-stimulated cells than in US cells ($n = 22$). The membrane/cytoplasm ratio of vinculin localization is significantly higher in ACh-stimulated cells than in US cells, but it is not significantly increased in FSK-stimulated cells.

to ACh but not FSK (Fig. 5, *A* and *B*). In contrast VASP undergoes phosphorylation at Ser^{157} in response to both ACh and FSK (Figs. 5*A* and 1, *A–C*).

Wild type vinculin or the phosphorylation deficient vinculin mutant Y1065F were expressed in ASM tissues to determine whether vinculin activation is required for the formation of VASP-vinculin complexes (Fig. 5, *C–G*). The interaction between VASP and vinculin was evaluated in tissue extracts by immunoprecipitation (Fig. 5, *C* and *D*). The amount of endogenous vinculin that co-precipitated with VASP increased significantly in response to ACh stimulation in sham-treated muscles and tissues expressing WT vinculin, but not in tissues expressing vinculin Y1065F (Fig. 5, *C* and *D*). The expression of vinculin Y1065F did not affect VASP Ser^{157} phosphorylation in response to ACh. Immunofluorescence analysis confirmed that the expression of EGFP vinculin Y1065F also had no effect on the localization of VASP phospho-Ser^{157} to the membrane (Fig. 5*E*).

PLA assays were used to evaluate the interaction of vinculin and VASP in freshly dissociated smooth muscle cells from tissues expressing vinculin Y1065F or WT vinculin (Fig. 5, *F* and *G*). Very few spots were detected in unstimulated cells. In cells expressing WT vinculin, stimulation with ACh resulted in a dramatic increase in the number of PLA spots at the cell membrane, indicating that ACh stimulates formation of protein complexes containing both VASP and vinculin. In the cells expressing vinculin Y1065F, there were markedly fewer spots indicating VASP-vinculin complexes, demonstrating that vinculin activation is required for the interaction of VASP with vinculin in membrane complexes (Fig. 5, *F* and *G*).

Stimulation with ACh but Not FSK Causes VASP-VASP Complex Formation at the Membrane—VASP can form tetrametric homo-oligomers through VASP-VASP binding interactions at its C terminus (11, 12). Although we could not probe specifically for VASP tetrameric homo-oligomers within the smooth muscle cells and tissues, we used PLA to assess for protein complexes containing multiple VASP molecules (VASP-VASP complexes) (Fig. 6). The effect of stimulation with ACh and FSK on VASP-VASP complex formation was investigated by using VASP phospho-Ser^{239} as a target for both +PLA and −PLA probes. VASP phospho-Ser^{239} was chosen as a target epitope for the PLA probes because stimulation with ACh does not cause a significant increase in phosphorylation at this site for the first 10 min (Fig. 6, *A* and *B*). Thus, an increase in the number of PLA spots detected after 5–10 min stimulation with ACh should reflect more VASP-VASP interactions rather than an increase in VASP Ser^{239} phosphorylation.

In cells stimulated for 10 min with ACh, VASP-VASP PLA spots were clearly observed on the membrane, but spots were barely evident in unstimulated cells (Fig. 6, *C* and *D*). In contrast, when PLA for VASP-VASP interactions was performed on cells stimulated with FSK for 10 min, very few PLA spots were observed (Fig. 6, *C* and *D*), even though FSK causes VASP Ser^{239} phosphorylation to increase by more than 5-fold within 10 min (Fig. 6, *A* and *B*). Thus, stimulation with ACh induced the formation of VASP-VASP complexes by membrane-localized VASP proteins, whereas stimulation with FSK did not. The fact that FSK induces a much higher level of VASP Ser^{239} phosphorylation than ACh confirms that an increase in the level of VASP Ser^{239} phosphorylation by itself does not result in an increase in the number of PLA spots.

The effect of VASP Ser^{157} phosphorylation on VASP-VASP complex formation was evaluated by PLA in cells expressing VASP S157A and VASP WT (Fig. 6, *E* and *F*). ACh-stimulated cells expressing VASP S157A had significantly fewer VASP-VASP PLA spots than cells expressing VASP WT, indicating that the expression of VASP S157A inhibits VASP-VASP complex formation in response to ACh. Thus, without Ser^{157} phos-

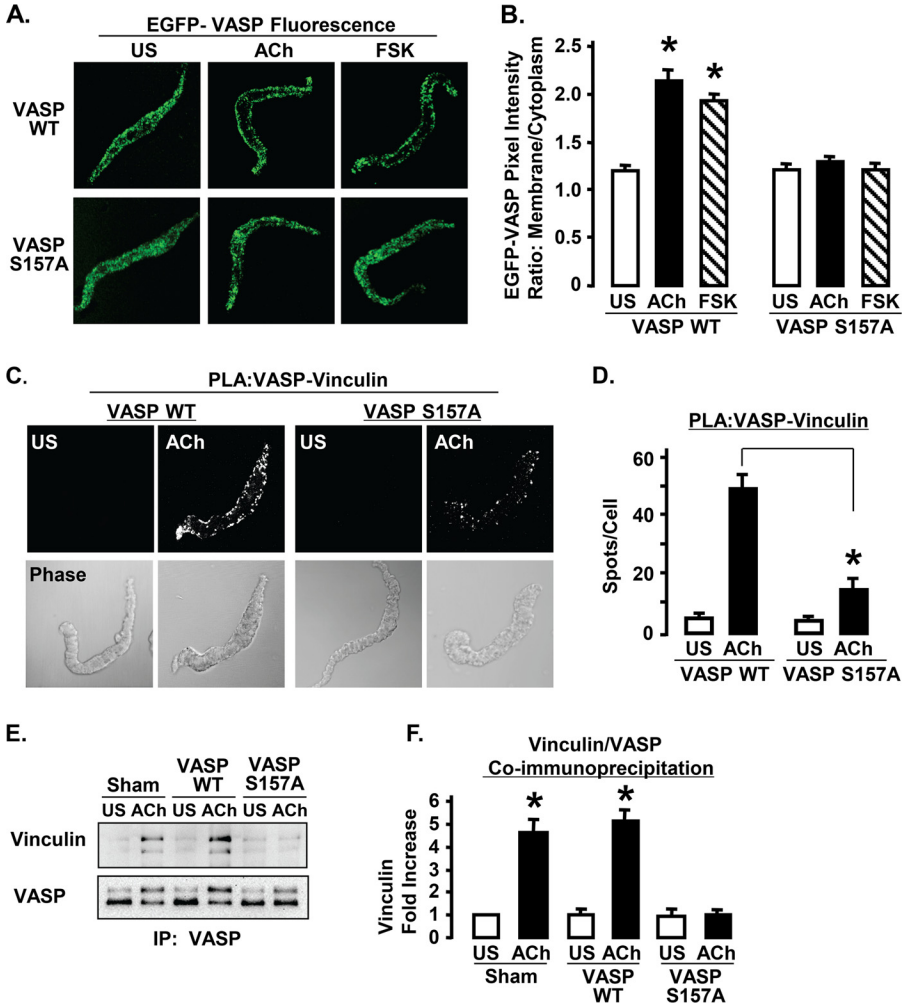

FIGURE 4. **Expression of EGFP VASP S157A inhibits the interaction of VASP and vinculin in response to ACh stimulation in ASM tissues.** *A,* localization of recombinant EGFP-VASP WT and EGFP VASP S157A in freshly dissociated ASM cells. Recombinant VASP was visualized in fixed cells by EGFP fluorescence. EGFP VASP WT localizes to the cell membrane in response to ACh or FSK stimulation, but EGFP VASP S157A is distributed throughout the cytoplasm and does not localize to the cell membrane after ACh or FSK stimulation. *B,* mean results for EGFP VASP WT and EGFP VASP S157A cellular localization in unstimulated (*US*), ACh-, or FSK-stimulated smooth muscle cells. Values represent the ratio of membrane to cytoplasmic pixel intensity for each cell. *, indicates significant difference from US cells ($n = 22–28$). *C, in situ* PLA were performed to visualize the interaction of vinculin with VASP in freshly dissociated ASM cells from tissues expressing VASP WT or VASP S157A. Each fluorescent spot indicates a complex between vinculin and VASP. *D,* mean results for effects of VASP WT ($n = 46$ cells) and VASP S157A ($n = 30$ cells) on the interaction of VASP and vinculin in US and ACh-stimulated cells. The expression of VASP S157A significantly reduces the interaction of VASP with vinculin in ACh-stimulated cells. *, significantly different. *E,* co-immunoprecipitation of vinculin after ACh stimulation was detected in VASP immunoprecipitates (*IP*) from tissues expressing VASP WT or sham treated, but not in tissues expressing VASP S157A. *F,* co-precipitation of vinculin with VASP increases significantly in sham-treated tissues and tissues expressing VASP WT but not in tissues expressing VASP S157A ($n = 4$).

phorylation, VASP does not form VASP-VASP complexes, probably because it does not localize to the membrane.

The effect of vinculin activation on VASP-VASP complex formation after stimulation with ACh was also evaluated by PLA using cells expressing either WT vinculin or vinculin Y1065F. There were significantly more PLA spots on the cell membrane cells expressing WT vinculin than in cells expressing vinculin Y1065F (Fig. 6, *G* and *H*). The results demonstrate that vinculin activation is required for the formation of VASP-VASP complexes at the cell membrane in response to stimulation with ACh. Although FSK stimulates VASP Ser^{157} phosphorylation, it does not stimulate vinculin activation, and thus FSK does not induce VASP-VASP complex formation.

Stimulation with ACh but Not FSK Increases the Interaction of VASP and Profilin at the Membrane—Profilin binds to VASP in its central proline-rich domain and is necessary for the transfer of G-actin monomers to the barbed ends of actin filaments by VASP (9). The effect of ACh and FSK on complex formation between VASP and profilin was evaluated using co-immunoprecipitation from tissue extracts and PLA in dissociated cells (Fig. 7). Stimulation with ACh but not FSK significantly increased the amount of profilin that co-immunoprecipitated with VASP compared with unstimulated tissues (Fig. 7, *A* and *B*). Significantly more PLA spots indicating VASP-profilin interactions were detected in ACh-stimulated cells than in FSK-stimulated or unstimulated cells (Fig. 7, *C* and *D*). These results indicate that ACh but not FSK induces the binding of profilin to VASP.

Vinculin Activation Is Required for the Formation of VASP-Profilin Complexes—WT vinculin and the phosphorylation deficient mutant vinculin Y1065F were expressed in ASM tissues to determine whether vinculin activation is required for the binding of profilin to VASP. The formation of complexes

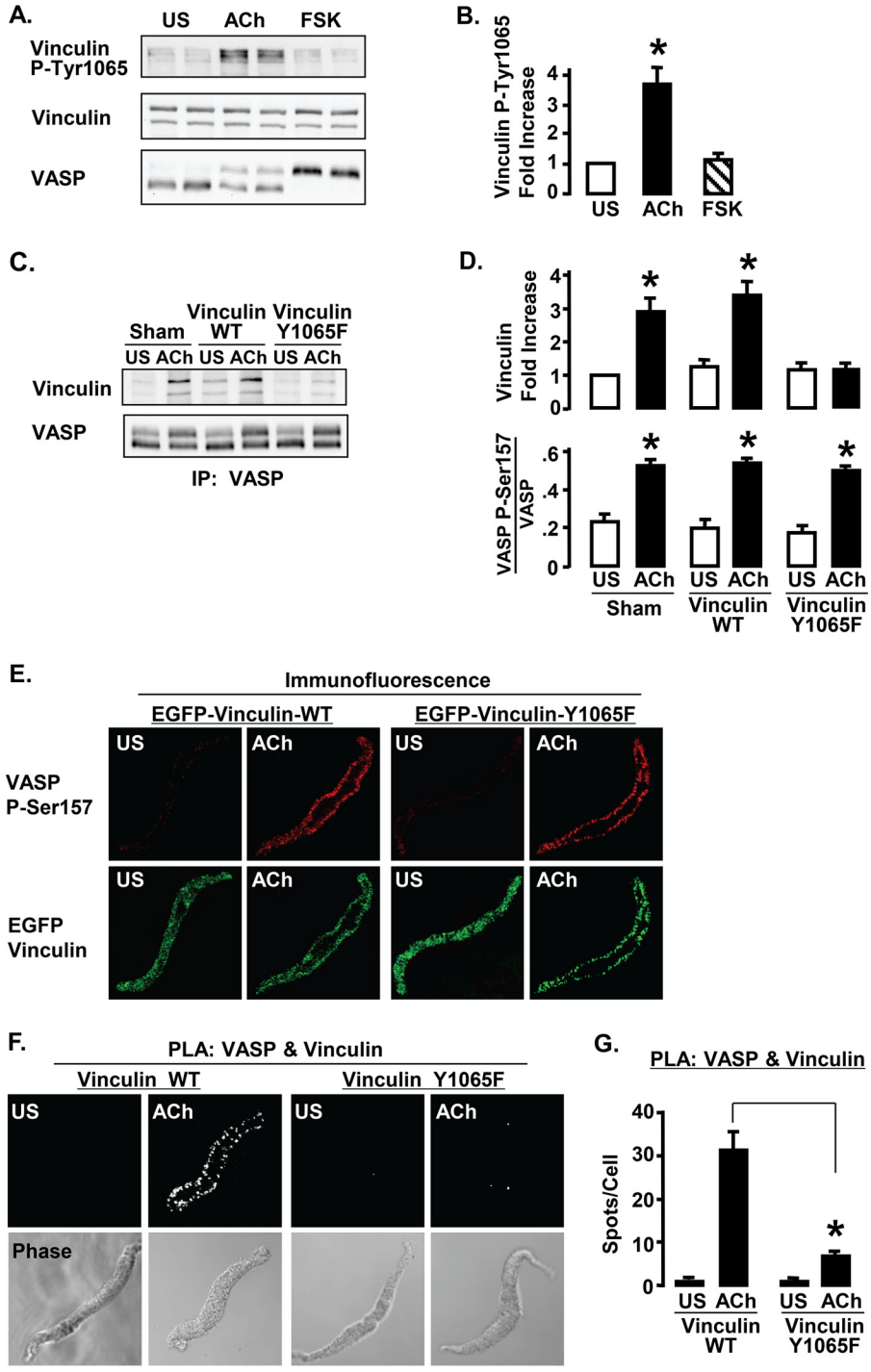

FIGURE 5. **Vinculin activation is required for the ACh-induced interaction of VASP with vinculin.** *A*, immunoblots of phospho-Tyr^{1065} vinculin and VASP from 6 ASM tissues stimulated with 10^{-4} M ACh, 10^{-6} M FSK, or unstimulated (*US*). ACh stimulation increases vinculin phosphorylation at Tyr^{1065}, but FSK has no effect on the vinculin Tyr^{1065} phosphorylation. VASP phosphorylation at Ser^{157} increases with both ACh and FSK stimulation. *B*, vinculin Tyr^{1065} phosphorylation increases significantly with ACh stimulation but not with FSK stimulation. *, significantly different from US ($n = 5$). *C*, co-precipitation of vinculin was observed in VASP immunoprecipitates (*IP*) after ACh stimulation of tissues expressing vinculin WT or sham-treated, but not in tissues expressing vinculin Y1065F. *D*, co-precipitation of vinculin with VASP increases significantly in sham-treated tissues and tissues expressing vinculin WT but not in tissues expressing vinculin Y1065F. VASP Ser^{157} phosphorylation increased significantly in response to ACh in all 3 treatment groups. *, significantly different from US ($n = 4$). *E*, localization of endogenous Ser^{157}-phosphorylated VASP in freshly dissociated ASM cells expressing EGFP vinculin Y1065F or EGFP WT vinculin. Cells were double stained for VASP phospho-Ser^{157} and GFP to visualize recombinant vinculin. In cells expressing either vinculin WT or vinculin Y1065F, endogenous Ser^{157}-phosphorylated VASP was localized on the membrane. Both EGFP-vinculin and vinculin Y1065F localize to the cell membrane in response to ACh. *F*, *in situ* PLA using VASP and vinculin antibodies were performed to visualize complexes between vinculin and VASP in freshly dissociated ASM cells from tissues expressing vinculin WT or vinculin Y1065F. Each fluorescent spot indicates interaction between vinculin and VASP. The interaction of VASP with vinculin in ACh-stimulated cells is inhibited in cells expressing vinculin Y1065F but not in cells expressing vinculin WT. *G*, mean number of PLA spots indicating vinculin-VASP complexes for each treatment. Significantly more spots were observed in ACh-stimulated cells expressing vinculin WT ($n = 23$) than in cells expressing vinculin Y1065F ($n = 27$). *, significant difference.

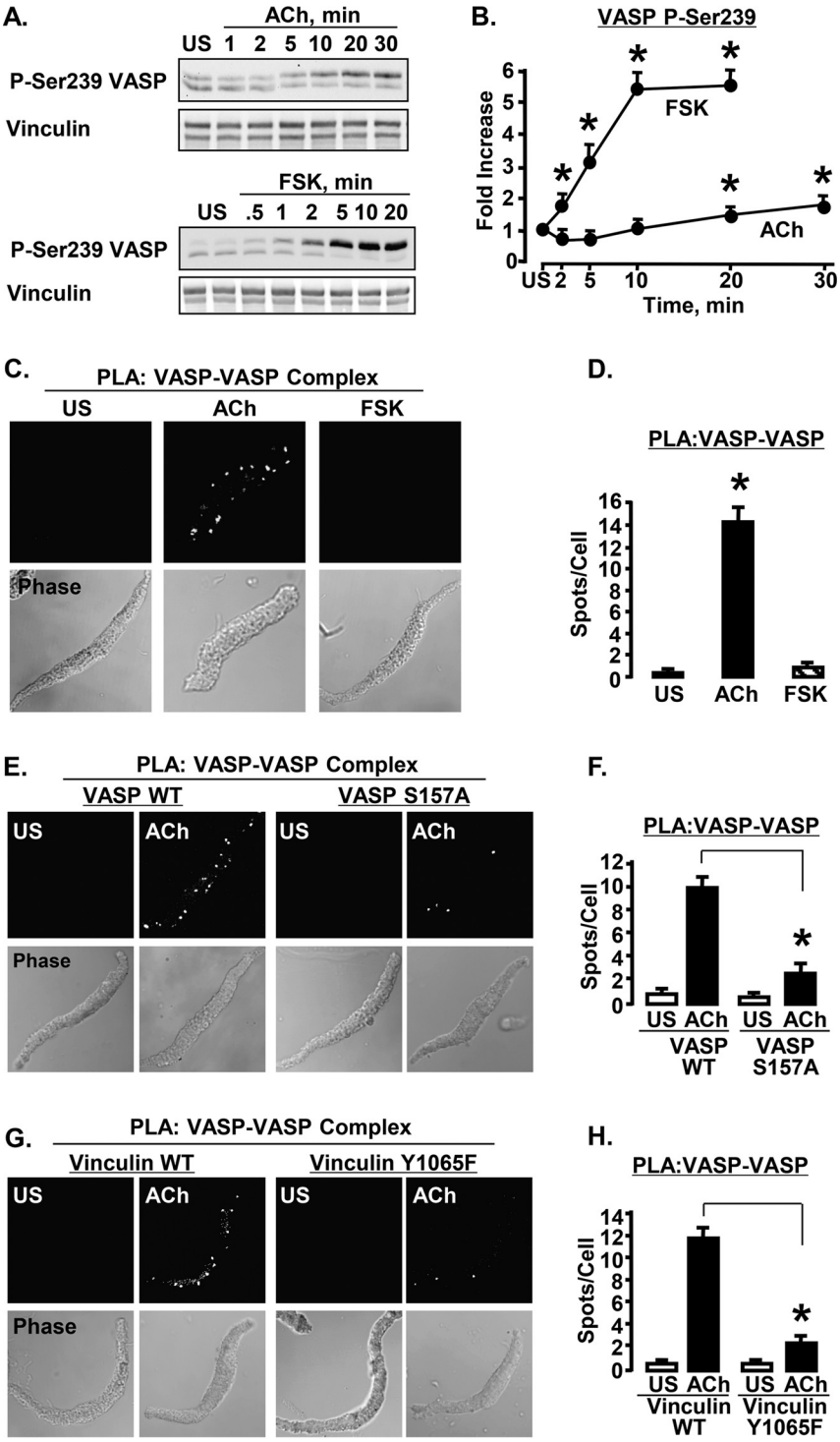

FIGURE 6. **Stimulation of ASM cells with ACh but not FSK induces VASP-VASP complex formation.** VASP-VASP complex formation is inhibited by the expression of VASP S157A or vinculin Y1065F. *A,* immunoblots of VASP Ser^{239} phosphorylation in tissue extracts in response to stimulation with ACh or FSK. Ser^{239}-phosphorylated VASP was detected in both bands of VASP using a site-specific Ser^{239} antibody. *B,* VASP Ser^{239} phosphorylation increased significantly more in response to FSK ($n = 7$) than in response to ACh ($n = 6$). (Values are fold-increase over unstimulated (*US*).) *, significantly greater than US. *C, in situ* PLA using VASP phospho-Ser^{239} mouse and rabbit antibodies to visualize VASP-VASP complex formation in freshly dissociated ASM cells. Each fluorescent spot indicates a VASP-VASP interaction. VASP complex formation increases in smooth muscle cells in response to ACh stimulation but not in response to FSK stimulation. *D,* mean results for VASP-VASP complex formation in response to FSK or ACh. *, significantly more PLA spots were observed at the membrane of the ACh-stimulated cells ($n = 21$) than in FSK-stimulated ($n = 29$) or US cells ($n = 22$). *E*, PLA was performed to visualize VASP-VASP complex formation in cells expressing VASP WT or VASP S157A. The expression of VASP S157A but not VASP WT inhibits VASP-VASP complex formation in ACh-stimulated cells. *F*, *, mean number of PLA spots was significantly higher in ACh-stimulated ASM cells expressing VASP WT ($n = 22$) than in cells expressing VASP S157A ($n = 25$). *G*, PLA was performed to visualize VASP-VASP complex formation in cells expressing vinculin WT or vinculin Y1065F. The expression of vinculin Y1065F but not vinculin WT inhibits VASP-VASP complex formation in ACh-stimulated cells. *H*, the total number of PLA spots was significantly higher in ACh-stimulated ASM cells expressing vinculin WT than in cells expressing vinculin Y1065F. *, mean number of PLA spots was significantly higher in ACh-stimulated ASM cells expressing vinculin WT ($n = 24$) than in cells expressing vinculin Y1065F ($n = 27$).

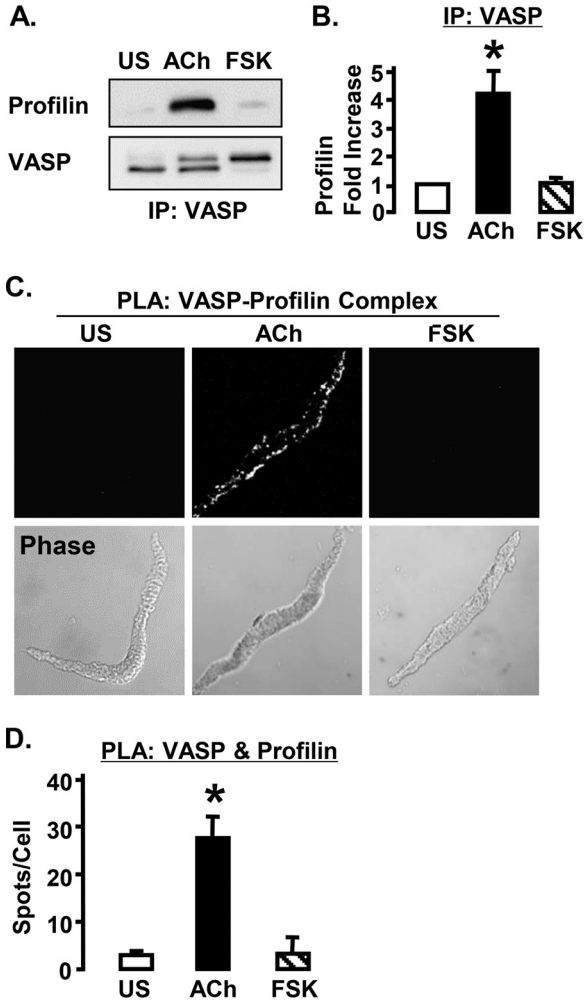

FIGURE 7. **ACh stimulation increases the interaction of profilin with VASP in ASM cells.** *A,* immunoblots from tissues stimulated with ACh, FSK, or unstimulated (*US*). Co-precipitation of profilin with VASP increases in response to stimulation with ACh but not with FSK. *B,* *, significantly more profilin co-precipitated with VASP from ACh-stimulated tissues than from US or FSK-stimulated tissues ($n = 3$). *C, in situ* PLA in freshly dissociated ASM cells to visualize the formation of complexes between profilin and VASP. Each fluorescent spot indicates a complex between profilin and VASP. *D,* *, significantly more PLA spots were observed in ACh-stimulated ASM cells ($n = 15$) than in FSK stimulated ($n = 18$) or US cells ($n = 18$). *IP*, immunoprecipitation.

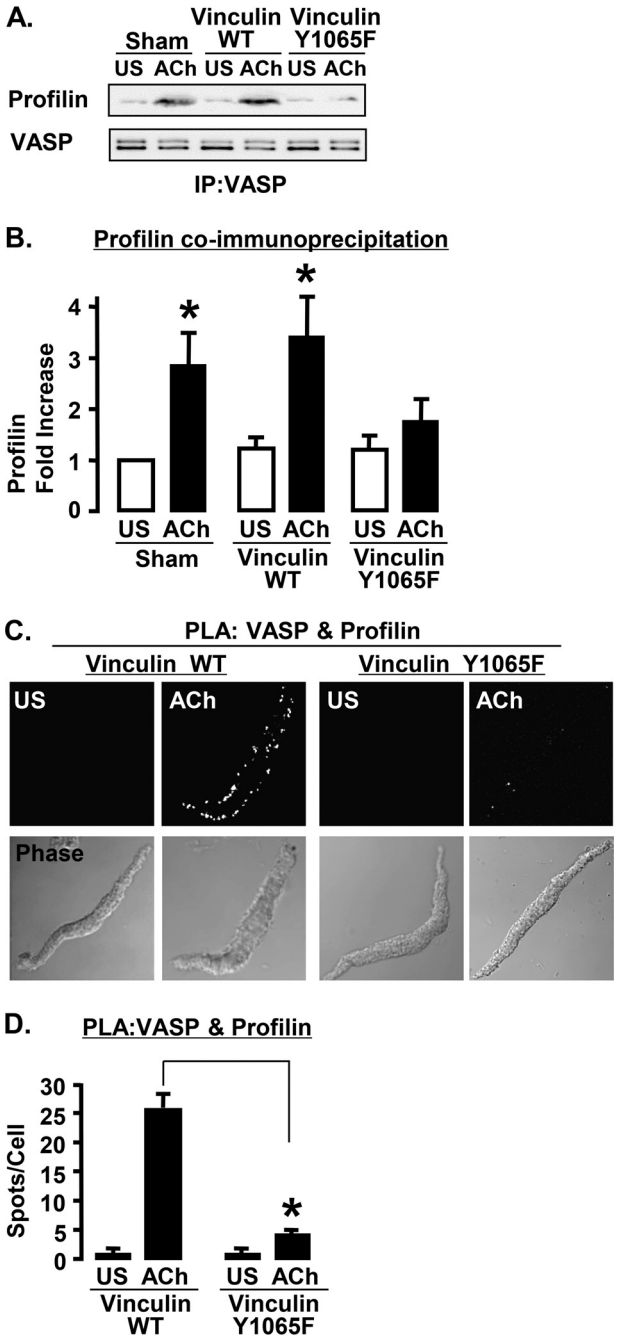

FIGURE 8. **Expression of vinculin Y1065F inhibits the VASP-profilin interaction.** *A,* immunoblots from VASP immunoprecipitates (*IP*) from tissues expressing vinculin WT, vinculin Y1065F, or sham-treated with or without ACh stimulation. *B,* the amount of profilin that co-precipitated with VASP during ACh stimulation increases significantly in sham-treated tissues and tissues expressing vinculin WT but not in tissues expressing vinculin Y1065F ($n = 5$). *, significantly different from US. *C,* PLA in cells expressing vinculin WT or vinculin Y1065F to visualize the formation of complexes between profilin and VASP. Each fluorescent spot indicates a complex between profilin and VASP. *D,* *, the total number of PLA spots was significantly higher in ACh-stimulated cells expressing vinculin WT ($n = 21$) than in cells expressing vinculin Y1065F ($n = 21$).

between VASP and profilin was evaluated by co-immunoprecipitation and PLA (Fig. 8). The amount of profilin that co-immunoprecipitated with VASP increased significantly in response to ACh stimulation in sham-treated muscles and tissues expressing WT vinculin, but not in tissues expressing vinculin Y1065F (Fig. 8, *A* and *B*). In cells expressing WT vinculin, stimulation with ACh resulted in a significant increase in the number of PLA spots along the cell membrane, indicating more interactions between VASP and profilin. In contrast, in the cells expressing vinculin Y1065F, there were significantly fewer spots at the membrane indicating VASP-profilin interactions. The results demonstrate that vinculin activation is prerequisite to the interaction of profilin with VASP at the membrane.

DISCUSSION

Our studies demonstrate that VASP is a critical regulator of actin dynamics and tension generation during the contractile stimulation of ASM (Fig. 2). Our results also indicate that the interaction of VASP with activated vinculin at membrane adhesion sites is a necessary prerequisite for VASP-mediated molecular processes that are required for actin polymerization (Figs. 5, 6, and 8). In ASM tissues, contractile stimulation triggered

the formation of VASP-VASP complexes at the membrane and also stimulated the interaction of profilin with VASP (Figs. 6–8). VASP oligomerization and its binding to profilin have been shown to be necessary steps in the VASP-mediated actin filament elongation process (7, 9); thus, our data are consistent with a function for VASP as an actin elongation factor during contractile stimulation.

We found that the stimulation of ASM with either ACh or FSK induces the phosphorylation of VASP on Ser^{157} (Fig. 1). The ACh-stimulated VASP Ser^{157} phosphorylation was mediated by PKC. We evaluated the role of VASP Ser^{157} phosphorylation on VASP activity by expressing the point mutant VASP S157A in ASM tissues. VASP S157A expression inhibited endogenous VASP phosphorylation on Ser^{157} and prevented the localization of VASP to the membrane in response to stimulation with either ACh or FSK (Figs. 2 and 4). When VASP localization to the membrane was prevented, actin polymerization and tension generation in response to contractile stimulation (ACh) were inhibited, but MLC phosphorylation was unaffected (Figs. 2 and 4). We have previously found that in ASM, the inhibition of actin polymerization does not affect the increase in MLC phosphorylation in response to ACh, but that tension generation is markedly reduced (2, 37). This suggests that MLC phosphorylation and actin polymerization are independently regulated and that both processes are necessary for tension development (1).

Although FSK induced VASP Ser^{157} phosphorylation and membrane localization, FSK did not stimulate actin polymerization (Fig. 2), the formation of VASP-VASP complexes (Fig. 6), or the interaction of profilin with VASP (Fig. 7). Thus, our results suggest that VASP Ser^{157} phosphorylation and membrane localization of VASP are necessary but not sufficient steps to initiate the activity of VASP in catalyzing actin polymerization.

We next evaluated the role of vinculin activation on the function of VASP in ASM tissues. We have previously shown that ACh stimulation induces the recruitment of vinculin to membrane adhesion complexes and vinculin activation (27, 28). In the present study, we found that FSK does not stimulate the recruitment of vinculin to the membrane (Fig. 3). Thus even though FSK stimulates the phosphorylation of VASP at Ser^{157} and the recruitment of VASP to the membrane, the phosphorylated VASP does not interact with vinculin.

We expressed the vinculin point mutant Y1065F in ASM tissues to determine the role of vinculin activation on the regulation of VASP activity. Using FRET technology, we previously demonstrated that the phosphorylation of vinculin on Tyr^{1065} is necessary for vinculin to sustain its activated ligand-binding conformation, and that the mutant vinculin Y1065F localizes to the membrane in a closed inactive conformation and inhibits the activation of endogenous vinculin (Fig. 5*E*) (27). In the present study, when vinculin activation was inhibited by the expression of vinculin Y1065F, contractile stimulation induced the phosphorylation of VASP on Ser^{157}; but VASP did not interact with vinculin (Fig. 5). Our observations suggest that even when both vinculin and VASP are localized at the membrane, VASP can only bind to vinculin when vinculin is in its open activated conformation. The inhibition of vinculin activation by the expression of vinculin Y1065F also prevented the formation of VASP-VASP complexes and the interaction of VASP with profilin (Figs. 6 and 8). These results suggest that vinculin activation and the binding of VASP to vinculin are necessary for VASP-mediated actin polymerization. The activation of vinculin may enable it to spatially and temporally coordinate the activity of VASP with other actin filament assembly promoting proteins.

The phosphorylation of VASP by cyclic nucleotide-dependent PKA and PKG protein kinases is well documented in multiple cell types including platelets, endothelial cells, and vascular and ASM cells (17, 19–21). PKC-dependent VASP Ser^{157} phosphorylation has been reported in vascular smooth muscle cells activated by serum stimulation (19, 43). Our findings are consistent with observations in migrating vascular endothelial cells that VASP phosphorylation on Ser^{157} provides a signal for VASP localization to the membrane or the leading edge of the cell (17, 19); however, these studies also reported that VASP Ser^{157} phosphorylation had a minor impact on actin polymerization. In contrast, we find that stimulus induced actin polymerization in ASM tissues requires the Ser^{157} phosphorylation of VASP (Fig. 2). However, our results suggest that this does not result from a direct effect of VASP phosphorylation on its actin catalytic activity; rather it results from the requirement that VASP localize to the membrane and bind to activated vinculin to initiate its actin catalytic function. We note that VASP Ser^{157} phosphorylation does not provide a reliable indicator of the VASP activation with respect to actin dynamics.

VASP has been shown to bind to the proline-rich motif in the hinge region of vinculin between its head and tail domains; whereas the binding sites for vinculin on VASP are located within its EVH1 domain (5, 29, 31, 44). Vinculin binding has also been proposed to mediate the recruitment of VASP to focal adhesion sites (29, 31). However, our studies demonstrate that in ASM, VASP recruitment to the membrane occurs in the absence of vinculin recruitment, and that the recruitment of VASP does not depend on vinculin activation or the interaction of VASP and vinculin. Our results are thus consistent with VASP Ser^{157} phosphorylation as a primary event in the regulation of VASP localization to adhesion junction complexes.

The assembly of VASP into tetrameric homo-oligomers is critical for the VASP-mediated process of actin filament elongation *in vitro* (4, 8, 13–15). Although VASP molecules self-assemble into stable tetramers *in vitro*; there is no evidence regarding the oligomerization state of VASP in living cells. We used a PLA to probe for multimeric VASP-VASP complexes in dissociated smooth muscle cells. Although PLA reports on complex formation between individual VASP proteins, it is not possible to confirm that the VASP protein complexes detected by PLA are tetramers. Other multimeric forms of VASP could be detected by PLA, as well as protein complexes that contain multiple VASP proteins or multimers bound in close proximity to an intermediary protein such as F-actin. *In vitro* studies have shown that VASP tetramers remain bound to the growing barbed ends of F-actin filaments during the elongation process (15). However, we observed few or no PLA spots in FSK-stimulated cells or in unstimulated cells, and there were also very few spots in ACh-stimulated cells treated with VASP S157A or

vinculin Y1065F. These observations are consistent with the possibility that VASP exists in a monomeric form in unstimulated cells and assembles into tetramers at membrane sites after ACh stimulation, and that the assembly of VASP tetramers is prerequisite to the functional role of VASP in actin dynamics.

PLA provides a very high resolution method for the detection of protein-protein interactions and protein complexes *in situ* (39, 40). We targeted the phospho-Ser^{239} epitope on VASP proteins using two different species antibodies; thus the PLA signal should reflect the interaction between at least two VASP monomers. The VASP Ser^{239} epitope was selected as a target because VASP Ser^{239} phosphorylation does not increase above basal levels within the first 10 min of ACh stimulation (Fig. 6*B*); therefore an increase in the PLA signal in response to ACh stimulation cannot reflect an increase in VASP Ser^{239} phosphorylation. In addition, although stimulation of the cells with FSK causes a 5–6-fold increase in VASP Ser^{239} phosphorylation (Fig. 6, *A* and *B*); no PLA signal for VASP-VASP complexes was detected in FSK-stimulated cells, which further confirms that an increase in VASP Ser^{239} phosphorylation does not cause an increase in the PLA signal (Fig. 6*C*). It remains possible that the VASP-VASP PLA signal reflects the formation of VASP multimeric complexes with other proteins in response to stimulation with ACh. However, if VASP is present primarily in tetrametric form in unstimulated cells, FSK-treated cells, and in cells treated with mutant VASP or vinculin, it is unclear why these VASP tetramers do not generate a PLA signal.

Our previous studies demonstrated that the actin polymerization catalyst N-WASp is important for the activation of actin polymerization by contractile agonists. We proposed that N-WASp-mediated actin polymerization is likely to occur in submembranous regions of the smooth muscle cell, and that these actin filaments are therefore most likely distinct from the actin filaments that participate in actomyosin cross-bridge cycling (1). VASP is known to catalyze actin polymerization by mechanisms that are different from those of N-WASp (4, 7). It is therefore possible that VASP regulates actin polymerization in a subset of actin filaments that are distinct from those regulated by N-WASp, and that VASP-mediated actin polymerization constitutes a separate pathway for actin remodelling in ASM (2). However, our data show that VASP-protein interactions that are necessary for its actin catalytic activity occur at adhesome junctions at the plasma membrane and not in the cytoplasm; VASP-mediated actin polymerization is most likely also confined to submembranous pools of actin at the cell cortex that are distinct from actin filaments in the contractile apparatus in the interior of the cell. Although contractile filament actin may undergo remodelling during ASM contraction and relaxation (45), mechanisms that might regulate the remodelling of cytoplasmic contractile actin have not yet been described.

Actin polymerization is recognized as an essential component of the cellular response to agonist stimulation in many smooth muscle cell types; however, its role in the cellular processes that regulate the activation of signaling pathways and the functional responses of the smooth muscle cells remain unclear. Cortical actin may serve a structural role to fortify linkages between the membrane junctional adhesome sites and actin filaments within the contractile apparatus. In this capacity, newly polymerized actin would serve to strengthen linkages between membrane junctional proteins such as α-actinin, vinculin, and talin and the actin filaments that interact with myosin to mediate cell shortening and tension development. Regulation of the connections between the contractile apparatus and the cell membrane could also serve to modify the orientation of the contractile filaments to adapt the cell to shape changes imposed by forces within its external environment. This could be particularly important in ASM, which is continuously subjected to changes in stress and strain during breathing (46). However, the function of cortical actin dynamics may not be entirely structural: cortical actin filaments may also provide a lattice for the assembly of junctional complexes that transduce signals from environmental stimuli to the interior of the cell. Although the function and regulation of actin cytoskeletal structures within smooth muscle remain to be established, dynamic remodelling of the actin cytoskeletal lattice is likely to serve multiple functions within the ASM cell.

REFERENCES

1. Gunst, S. J., and Zhang, W. (2008) Actin cytoskeletal dynamics in smooth muscle: a new paradigm for the regulation of smooth muscle contraction. *Am. J. Physiol. Cell. Physiol.* **295,** C576-C587
2. Zhang, W., Wu, Y., Du, L., Tang, D. D., and Gunst, S. J. (2005) Activation of the Arp2/3 complex by N-WASp is required for actin polymerization and contraction in smooth muscle. *Am. J. Physiol. Cell. Physiol.* **288,** C1145-C1160
3. Higgs, H. N., and Pollard, T. D. (1999) Regulation of actin polymerization by Arp2/3 complex and WASp/Scar proteins. *J. Biol. Chem.* **274,** 32531–32534
4. Kwiatkowski, A. V., Gertler, F. B., and Loureiro, J. J. (2003) Function and regulation of Ena/VASP proteins. *Trends Cell Biol.* **13,** 386–392
5. Bear, J. E., and Gertler, F. B. (2009) Ena/VASP: towards resolving a pointed controversy at the barbed end. *J. Cell Sci.* **122,** 1947–1953
6. Bear, J. E., Svitkina, T. M., Krause, M., Schafer, D. A., Loureiro, J. J., Strasser, G. A., Maly, I. V., Chaga, O. Y., Cooper, J. A., Borisy, G. G., and Gertler, F. B. (2002) Antagonism between Ena/VASP proteins and actin filament capping regulates fibroblast motility. *Cell* **109,** 509–521
7. Dominguez, R. (2009) Actin filament nucleation and elongation factors: structure-function relationships. *Crit. Rev. Biochem. Mol. Biol.* **44,** 351–366
8. Breitsprecher, D., Kiesewetter, A. K., Linkner, J., Vinzenz, M., Stradal, T. E., Small, J. V., Curth, U., Dickinson, R. B., and Faix, J. (2011) Molecular mechanism of Ena/VASP-mediated actin-filament elongation. *EMBO J.* **30,** 456–467
9. Ferron, F., Rebowski, G., Lee, S. H., and Dominguez, R. (2007) Structural basis for the recruitment of profilin-actin complexes during filament elongation by Ena/VASP. *EMBO J.* **26,** 4597–4606
10. Haffner, C., Jarchau, T., Reinhard, M., Hoppe, J., Lohmann, S. M., and Walter, U. (1995) Molecular cloning, structural analysis and functional expression of the proline-rich focal adhesion and microfilament-associated protein VASP. *EMBO J.* **14,** 19–27
11. Zimmermann, J., Labudde, D., Jarchau, T., Walter, U., Oschkinat, H., and Ball, L. J. (2002) Relaxation, equilibrium oligomerization, and molecular symmetry of the VASP(336–380) EVH2 tetramer. *Biochemistry* **41,** 11143–11151
12. Bachmann, C., Fischer, L., Walter, U., and Reinhard, M. (1999) The EVH2 domain of the vasodilator-stimulated phosphoprotein mediates tetramerization, F-actin binding, and actin bundle formation. *J. Biol. Chem.* **274,** 23549–23557
13. Kühnel, K., Jarchau, T., Wolf, E., Schlichting, I., Walter, U., Wittinghofer, A., and Strelkov, S. V. (2004) The VASP tetramerization domain is a right-handed coiled coil based on a 15-residue repeat. *Proc. Natl. Acad. Sci.*

U.S.A. **101,** 17027–17032
14. Hansen, S. D., and Mullins, R. D. (2010) VASP is a processive actin polymerase that requires monomeric actin for barbed end association. *J. Cell Biol.* **191,** 571–584
15. Breitsprecher, D., Kiesewetter, A. K., Linkner, J., Urbanke, C., Resch, G. P., Small, J. V., and Faix, J. (2008) Clustering of VASP actively drives processive, WH2 domain-mediated actin filament elongation. *EMBO J.* **27,** 2943–2954
16. Gertler, F. B., Niebuhr, K., Reinhard, M., Wehland, J., and Soriano, P. (1996) Mena, a relative of VASP and *Drosophila* Enabled, is implicated in the control of microfilament dynamics. *Cell* **87,** 227–239
17. Benz, P. M., Blume, C., Seifert, S., Wilhelm, S., Waschke, J., Schuh, K., Gertler, F., Münzel, T., and Renné, T. (2009) Differential VASP phosphorylation controls remodeling of the actin cytoskeleton. *J. Cell Sci.* **122,** 3954–3965
18. Blume, C., Benz, P. M., Walter, U., Ha, J., Kemp, B. E., and Renné, T. (2007) AMP-activated protein kinase impairs endothelial actin cytoskeleton assembly by phosphorylating vasodilator-stimulated phosphoprotein. *J. Biol. Chem.* **282,** 4601–4612
19. Döppler, H., and Storz, P. (2013) Regulation of VASP by phosphorylation: consequences for cell migration. *Cell Adh. Migr.* **7,** 482–486
20. Kim, H. R., Graceffa, P., Ferron, F., Gallant, C., Boczkowska, M., Dominguez, R., and Morgan, K. G. (2010) Actin polymerization in differentiated vascular smooth muscle cells requires vasodilator-stimulated phosphoprotein. *Am. J. Physiol. Cell. Physiol.* **298,** C559-C571
21. Goncharova, E. A., Goncharov, D. A., Zhao, H., Penn, R. B., Krymskaya, V. P., and Panettieri, R. A., Jr. (2012) β2-Adrenergic receptor agonists modulate human airway smooth muscle cell migration via vasodilator-stimulated phosphoprotein. *Am. J. Respir. Cell Mol. Biol.* **46,** 48–54
22. Freyer, A. M., Billington, C. K., Penn, R. B., and Hall, I. P. (2004) Extracellular matrix modulates β2-adrenergic receptor signaling in human airway smooth muscle cells. *Am. J. Respir. Cell Mol. Biol.* **31,** 440–445
23. Zhang, W., and Gunst, S. J. (2008) Interactions of airway smooth muscle cells with their tissue matrix: implications for contraction. *Proc. Am. Thorac. Soc.* **5,** 32–39
24. Humphries, J. D., Wang, P., Streuli, C., Geiger, B., Humphries, M. J., and Ballestrem, C. (2007) Vinculin controls focal adhesion formation by direct interactions with talin and actin. *J. Cell Biol.* **179,** 1043–1057
25. Ziegler, W. H., Liddington, R. C., and Critchley, D. R. (2006) The structure and regulation of vinculin. *Trends Cell Biol.* **16,** 453–460
26. Johnson, R. P., and Craig, S. W. (1994) An intramolecular association between the head and tail domains of vinculin modulates talin binding. *J. Biol. Chem.* **269,** 12611–12619
27. Huang, Y., Day, R. N., and Gunst, S. J. (2014) Vinculin phosphorylation at Tyr^{1065} regulates vinculin conformation and tension development in airway smooth muscle tissues. *J. Biol. Chem.* **289,** 3677–3688
28. Huang, Y., Zhang, W., and Gunst, S. J. (2011) Activation of vinculin induced by cholinergic stimulation regulates contraction of tracheal smooth muscle tissue. *J. Biol. Chem.* **286,** 3630–3644
29. Brindle, N. P., Holt, M. R., Davies, J. E., Price, C. J., and Critchley, D. R. (1996) The focal-adhesion vasodilator-stimulated phosphoprotein (VASP) binds to the proline-rich domain in vinculin. *Biochem. J.* **318,** 753–757
30. Quinlan, M. P. (2004) Vinculin, VASP, and profilin are coordinately regulated during actin remodeling in epithelial cells, which requires *de novo* protein synthesis and protein kinase signal transduction pathways. *J. Cell. Physiol.* **200,** 277–290
31. Hüttelmaier, S., Mayboroda, O., Harbeck, B., Jarchau, T., Jockusch, B. M., and Rüdiger, M. (1998) The interaction of the cell-contact proteins VASP and vinculin is regulated by phosphatidylinositol-4,5-bisphosphate. *Curr. Biol.* **8,** 479–488
32. Cohen, D. M., Chen, H., Johnson, R. P., Choudhury, B., and Craig, S. W. (2005) Two distinct head-tail interfaces cooperate to suppress activation of vinculin by talin. *J. Biol. Chem.* **280,** 17109–17117
33. Tang, D. D., Turner, C. E., and Gunst, S. J. (2003) Expression of non-phosphorylatable paxillin mutants in canine tracheal smooth muscle inhibits tension development. *J. Physiol.* **553,** 21–35
34. Zhang, W., Huang, Y., and Gunst, S. J. (2012) The small GTPase RhoA regulates the contraction of smooth muscle tissues by catalyzing the assembly of cytoskeletal signaling complexes at membrane adhesion sites. *J. Biol. Chem.* **287,** 33996–34008
35. Opazo Saez A., Zhang, W., Wu, Y., Turner, C. E., Tang, D. D., and Gunst, S. J. (2004) Tension development during contractile stimulation of smooth muscle requires recruitment of paxillin and vinculin to the membrane. *Am. J. Physiol. Cell Physiol* **286,** C433-C447
36. Zhang, W., and Gunst, S. J. (2006) Dynamic association between α-actinin and β-integrin regulates contraction of canine tracheal smooth muscle. *J. Physiol.* **572,** 659–676
37. Mehta, D., and Gunst, S. J. (1999) Actin polymerization stimulated by contractile activation regulates force development in canine tracheal smooth muscle. *J. Physiol.* **519**, 829–840
38. Hathaway, D. R., and Haeberle, J. R. (1985) A radioimmunoblotting method for measuring myosin light chain phosphorylation levels in smooth muscle. *Am. J. Physiol.* **249,** C345-C351
39. Söderberg, O., Gullberg, M., Jarvius, M., Ridderstråle, K., Leuchowius, K. J., Jarvius, J., Wester, K., Hydbring, P., Bahram, F., Larsson, L. G., and Landegren, U. (2006) Direct observation of individual endogenous protein complexes in situ by proximity ligation. *Nat. Methods* **3,** 995–1000
40. Söderberg, O., Leuchowius, K. J., Gullberg, M., Jarvius, M., Weibrecht, I., Larsson, L. G., and Landegren, U. (2008) Characterizing proteins and their interactions in cells and tissues using the *in situ* proximity ligation assay. *Methods* **45,** 227–232
41. Butt, E., Abel, K., Krieger, M., Palm, D., Hoppe, V., Hoppe, J., and Walter, U. (1994) cAMP- and cGMP-dependent protein kinase phosphorylation sites of the focal adhesion vasodilator-stimulated phosphoprotein (VASP) *in vitro* and in intact human platelets. *J. Biol. Chem.* **269,** 14509–14517
42. Wentworth, J. K., Pula, G., and Poole, A. W. (2006) Vasodilator-stimulated phosphoprotein (VASP) is phosphorylated on Ser157 by protein kinase C-dependent and -independent mechanisms in thrombin-stimulated human platelets. *Biochem. J.* **393,** 555–564
43. Chitaley, K., Chen, L., Galler, A., Walter, U., Daum, G., and Clowes, A. W. (2004) Vasodilator-stimulated phosphoprotein is a substrate for protein kinase C. *FEBS Lett.* **556,** 211–215
44. Reinhard, M., Rüdiger, M., Jockusch, B. M., and Walter, U. (1996) VASP interaction with vinculin: a recurring theme of interactions with proline-rich motifs. *FEBS Lett.* **399,** 103–107
45. Herrera, A. M., Martinez, E. C., and Seow, C. Y. (2004) Electron microscopic study of actin polymerization in airway smooth muscle. *Am. J. Physiol. Lung Cell. Mol. Physiol.* **286,** L1161-L1168
46. Gunst, S. J., Tang, D. D., and Opazo Saez, A. (2003) Cytoskeletal remodeling of the airway smooth muscle cell: a mechanism for adaptation to mechanical forces in the lung. *Respir. Physiol. Neurobiol.* **137,** 151–168